FINAL REPORT

NASA GRANT NAG8-767

GROWTH OF ZINC SELENIDE CRYSTALS BY PHYSICAL VAPOR TRANSPORT IN MICROGRAVITY

Period of Performance
4/1/89 - 8/31/95

Principal Investigator
FRANZ ROSENBERGER

Center for Microgravity and Materials Research
University of Alabama in Huntsville
Huntsville, Alabama 35899

Table of Contents

1. Executive Summary 1
2. Background 1
   - 2.1. Zinc selenide 1
   - 2.2. Zinc sulfide 2
   - 2.3. Zinc sulfoselenide 3
   - 2.4. Seed orientation 3
   - 2.5. Cadmium telluride 4
3. Approach and Techniques 4
4. Results and Discussion 9
5. Conclusions 11
6. References 14

1. Executive Summary

The growth of single crystals of zinc selenide was carried out by both closed ampoule physical vapor transport and effusive ampoule physical vapor transport (EAPVT). The latter technique was shown to be a much more efficient method for the seeded growth of zinc selenide, resulting in higher transport rates. Furthermore, EAPVT work on CdTe has shown that growth onto {n11} seeds is advantageous for obtaining reduced twinning and defect densities in II-VI sphalerite materials.

2. Background

2.1 Zinc selenide

Single crystals of zinc selenide and zinc sulfoselenide are important for optical device applications [1]. Zinc sulfoselenide is miscible for all compositions,of the quasi binary system, and zinc sulfide has the largest band gap of any II-VI compound. Discovery of the zinc selenide semiconductor laser [2-4] has dramatically increased interest in zinc selenide and zinc sulfoselenide single crystals. Yet, the most important uses for $ZnS_{1-x}Se_x$ bulk single crystals are as substrates for optoelectronic transistors [5], although there are other optoelectronic uses, such as p-n junction LEDs [6]. These substrates do not have the problems of heterosystems, such as $ZnSe_{0.95}S_{0.05}$ on GaAs [7,8] or ZnS on Si [9] with respect to thermal expansion or diffusion and chemical reactions along the junction. However, in view of the high price of zinc sulfoselenide substrates, the quality of epitaxial layers obtained on this material must be much

higher than that of epitaxial layers on GaAs or Si substrates, in order to make this approach economically feasible.

Zinc selenide single crystals have been grown by a wide variety of methods including melt growth, chemical and physical vapor growth, solution growth and hydrothermal growth; see, e. g. [10-14]. Polytypism has never been reported in these crystals and twinning occurs less often than in zinc sulfide or sulfoselenide (see below). The wurtzite-sphalerite transition temperature for zinc selenide is approximately 1425 °C [15].

As a consequence of this high transition temperature, growth temperatures can be chosen higher than in zinc sulfide or zinc sulfoselenide. Thus higher growth rates can be obtained. Growth rates from the melt are up to 5 mm/hr [13], higher than any other method, but there are a number of problems with twinning and other defects that limit the uses of crystals produced by this method [16]. Zinc selenide crystals grown by the Bridgman technique have about 10^2 times more dislocations per cm^2 than crystals grown from the vapor [14,17-19], as well as 8 times wider X-ray diffraction lines at half-maximum [14]. In crystals grown from the vapor with rates of 5 mm/day, etch-pit counts indicate dislocation densities often as low as $10^4/cm^2$[10,18].

Since below 1100 °C (a typical temperature limit for standard laboratory furnaces) physical vapor transport rates are low, chemical vapor transport was often used at these temperatures. With iodine transport at 900 °C, growth rates were enhanced up to four times [20]. However, the iodine was incorporated into the crystal at levels of 200 to 500 ppm [18, 21], resulting in n-type material. Even after treatment in molten zinc, iodine transported crystals showed a sevenfold increase in the conductivity (350 $mho \cdot cm^{-1}$) [18] as compared to physical vapor transported samples. Crystals grown by chlorine transport contained about ten parts per million of chlorine and had six orders of magnitude higher conductivity (10^{-6} $mho \cdot cm^{-1}$) than physical vapor transported zinc selenide samples [22]. In addition, X-ray diffraction showed that iodine in zinc selenide causes an increase in the lattice constant of 10^{-3} Å per 50 ppm [21]. Less twinning within the crystal has also been reported [10,18], although it is not clear whether this was caused by iodine incorporation, or the higher transport flux it created.

2.2 Zinc Sulfide

Zinc sulfide sphalerite crystal growth faces serious problems with respect to polytypism and twinning [20,23-28]. A variety of explanations have been proposed for polytypism [29,30] in which a mixture of crystal phases coexists in the same crystals. In zinc sulfide powder, a sphalerite-wurtzite transition has been observed at approximately 1020 °C [31]. However, Baars and Brandt [32] have shown that bulk crystals of zinc sulfide do not change structure at this

temperature. Instead, they found that a sphalerite crystal would remain in that structure for a temperature region above the powder transition temperature, then gradually transform to the wurtzite structure as the temperature continued to rise. If the crystal was then cooled, it did not start to transform back to the sphalerite structure until it was well beneath the powder transition temperature. The transformation from wurtzite to sphalerite is not completed at low temperatures, but only during reheating, indicating that at low temperatures the transformation is kinetically frozen.

Both Russell and Woods [28] and Paloszet al. [20,25] found lesser amounts of polytypism by X-ray measurements in zinc sulfide crystals grown beneath the sphalerite-wurtzite transition temperature than in crystals grown right above the transition temperature. Crystals grown at or below 900 °C have almost no polytypism when grown at 1 mm/day or less [20]. The low growth rate becomes a serious problem for the production of bulk crystals. Above 1100 °C, zinc sulfide crystals grow much faster [27]. Baars and Brandt [32] showed by high-temperature X-ray diffraction that growth at this temperature results in a pure wurtzite crystal. Yet they found it difficult to cool these crystals quickly enough to prevent the formation of polytypes. Only small platelets grown at this temperature have been reported in the wurtzite structure at room temperature without heavy disorder.

2.3 Zinc sulfoselenide

Less is known about growth conditions and resulting properties of zinc sulfoselenide than for either zinc selenide of zinc sulfide. In particular, the wurtzite-sphalerite transition temperature has not been determined for zinc sulfoselenide. One can only draw on information from similar alloys. For instance, in the cadmium zinc selenide system, which also forms a continuous set of solid solutions, cadmium selenide has a much lower transition temperature than zinc selenide. Kulakov and Balyakina [15] found that the cadmium zinc selenide wurtzite-sphalerite transition temperature decreased as more cadmium replaced zinc in the crystal. If the same trend holds for zinc sulfoselenide, replacing some of the sulfur in the zinc sulfide with selenium should increase the transition temperature. In both zinc sulfide and selenide, the disorder is reduced with an increasing difference between the growth and transition temperatures. Hence, one could expect that zinc sulfoselenide crystals grown at the same temperatures with greater selenium concentrations could have reduced disorder. This has been partially confirmed in the studies of both Catano and Kun [21] and Russell and Woods [27,28]. In both of these studies, the amount of twinning and defects increased with increasing sulfur concentration.

2.4. Seed Orientation

In all three materials, little is known about the best seed (growth face) orientation that

results in minimum twinning and dislocationformation. Some research on III-V sphalerite structure materials suggest that {211} or other {n11} faces are optimal for this purpose [33,34].

2.5. Cadmium Telluride

At a later stage during this investigation, when the PI of grant NAG8-767 retired, it became apparent that the most advantageous material for testing the concept of EAPVT, as well as studying the influence of the seed orientation on defect formation, was cadmium telluride. The reduced compositional complexity, as well as a much larger data base existing for this material made it more advantageous for the ensuing investigations. Furthermore, with approval of the technical grant monitors at MSFC, it was decided to pool the remaining funds of grants NAG8-767 and NAG8-842 for the CdTe growth project. Hence, the same final report is submitted for these grants.

The relevant background information on CdTe is provided in the respective parts of the Approach and Techniques, and Results sections. This allows for more ready interpretations of the findings.

3. Approach and Techniques

Originally, zinc selenide and zinc sulfoselenide crystal growth was to have been studied using physical vapor transport in closed ampoules. The geometry of the ampoules used is shown in Figure 1. After the source material was placed in the ampoule, the ampoule was evacuated and the tube sealed off. Some centimeter-plus crystals of zinc selenide were obtained in these closed ampoules [19]. Crystals from these earlier zinc selenide experiments included several cm^3-sized boules that were mostly single crystal. The dislocation densities in these crystals, determined by a bromine in methanol etchant, were roughly $10^4/cm^2$. $ZnS_{0.8}Se_{0.2}$ crystals obtained in these earlier experiments had a dislocation density of roughly $10^6/cm^2$. These crystals had numerous twins and grain boundaries.

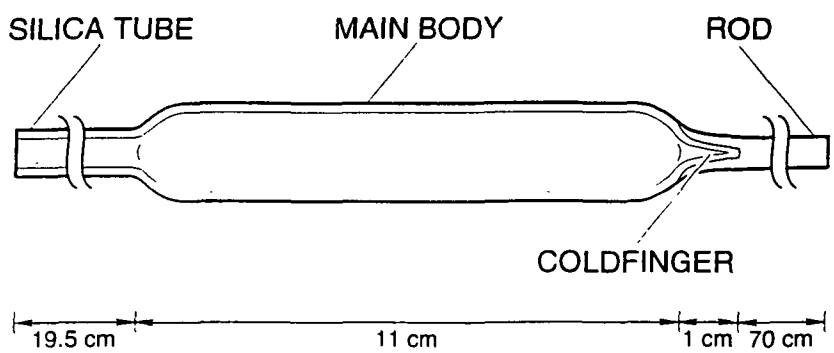

Figure 1. Physical Vapor transport closed ampoule

Continuation of these growth experiments (after retirement of the original PI and departure of the postdoctoral research associate) with zinc sulfoselenide revealed extensive problems with wall nucleation and slow transport of material. Transport rates dropped as much as eighty percent. Hence, it was decided to move to the effusive ampoule physical vapor transport (EAPVT) method to increase growth rates, and to use a high-temperature microscope to view the crystal during growth without causing a large variation in the temperature profile.

In contrast to sealed ampoule vapor growth, in EAPVT, excess (incongruent) components and other transport-limiting vapor constituents are continuously removed to vacuum. Model calculations [35,36], and previous experiments [37,38] with this technique showed that impurities are removed most efficiently when the leak is positioned in close proximity of the crystal, and that the leak rate can be as low as 2-5% of the sublimation flux to maintain diffusionless (quasi-congruent) transport. Since no sealing is required, ground joints are used to connect the various parts of the reusable ampoule. Thus, the ampoule can readily be closed, without having to expose seeds and starting material to the high temperature required for silica fusion sealing.

The quasi-congruent vapor composition achieved by EAPVT leads to vapor flow that is limited only by viscous interaction with the ampoule wall. Thus, even for small ΔT's between the source and crystal, transport proceeds too rapidly to result in single crystalline condensation. Therefore, a flow-restricting capillary is placed between the source and crystal to ensure crystal growth of high structural quality. The dimensions of this capillary are calculated using the Hagen-Poiseuille relation for viscous flow in cylindrical tubes. This predetermination of the vapor flow from the source to the crystal is based on ΔT's (and corresponding vapor pressures) that are large compared to temperature instabilities associated with the furnace controllers, but small compared to ΔT's required in closed ampoule vapor transport. This assures steady transport and growth, while facilitating the minimization of temperature gradients in the system.

Previous work on CdTe using the effusive ampoule technique included both self-nucleated and seeded growth [38, 39]. Since available seeds had etch pit densities (EPD's) of 10^4-$10^5/cm^2$, self-nucleated growth was conducted first. These growth runs resulted in about 10 grains arranged in a radial pattern. The grains, which grew approximately in <110> directions, were highly twinned and had high EPD's.

The use of seeds resulted in fewer defects and enabled predetermination of the crystal orientation. {111} and {110} seeds were used. Lateral growth from the seed proceeded without formation of twins or grain boundaries and typical EPD's of $2\times10^3/cm^2s$. Growth rates on the

seeds were 0.5 to 1.2 cm/day. Precipitates formed primarily along grain and twin boundaries; large areas (1 cm^2) were free of precipitates. The limit of resolution for detecting precipitates was approximately 1 micron. Nearly theoretical transmissivities were obtained between 860 and 3200 nm.

However, the crystallographic quality of crystals grown in this first furnace deteriorated with distance from the seed. This was caused by too high temperature gradients resulting from an inadequate thermal design of the furnace. An obvious manifestation of these gradients was the saddle shape of the crystals, with the orientation of the highest parts towards the viewports, indicating too high radiation losses in these directions.

Hence, a crystal growth system was designed to provide:

- Continuous removal of gaseous impurities and excess components to reproducibly obtain rapid transport.
- Means of limiting the transport flux to values that ensure low-defect single crystal growth.
- Direct viewing of the crystal-vapor interface to monitor nucleation conditions, etching of seed plates, growth rates and morphologies.
- A temperature difference between the source and crystal interface that is much larger than any temperature fluctuations due to the furnace-controller system, so that steady crystal growth can occur.
- Somewhat independent adjustment of the temperatures of the seed pedestal and in the vapor in front of the crystal, in order to ensure morphological stability of the growing interface and suppress parasitic nucleation.
- Minimization of axial and radial temperature gradients in the crystal during growth and cooldown.
- Smooth movement of the ampoule within the heating elements to continuously obtain steady growth without significantly changing the position of the interface in the temperature profile.
- A furnace shell with defined heat losses, in order to facilitate optimal temperature control.
- Monitoring of growth conditions to ensure reproducibility and aid in troubleshooting.

In order to perform these tasks, a new furnace with three independently controlled heating elements was designed. A lightpipe is used to cool the seed and growing crystal through the seed pedestal. The viewing ports are designed to minimize heat losses. An integrated high-temperature microscope allows for direct viewing of the seed. An attached vacuum system provides the low pressure needed for the effusive ampoule method. In order to prevent contamination of the growth atmosphere by hydrocarbons, a turbomolecular pump is used. The ampoule/capillary geometry is designed such that variations in temperature are less than 1% of

the ΔT between the source and the growing crystal. Precise temperature control is facilitated by cooling the outer shell of the furnace to a low, reasonably constant temperature. A programmable stepping motor moves the furnace in 1 micron steps. To assure reproducibility, a PC is used to program the temperatures and translation rates, and to continuously record the furnace temperatures and the pressure in the vacuum system.

The resulting growth ampoule and EAPVT setup, that incorporate the above design features are depicted in Figure 2 and 3, respectively.

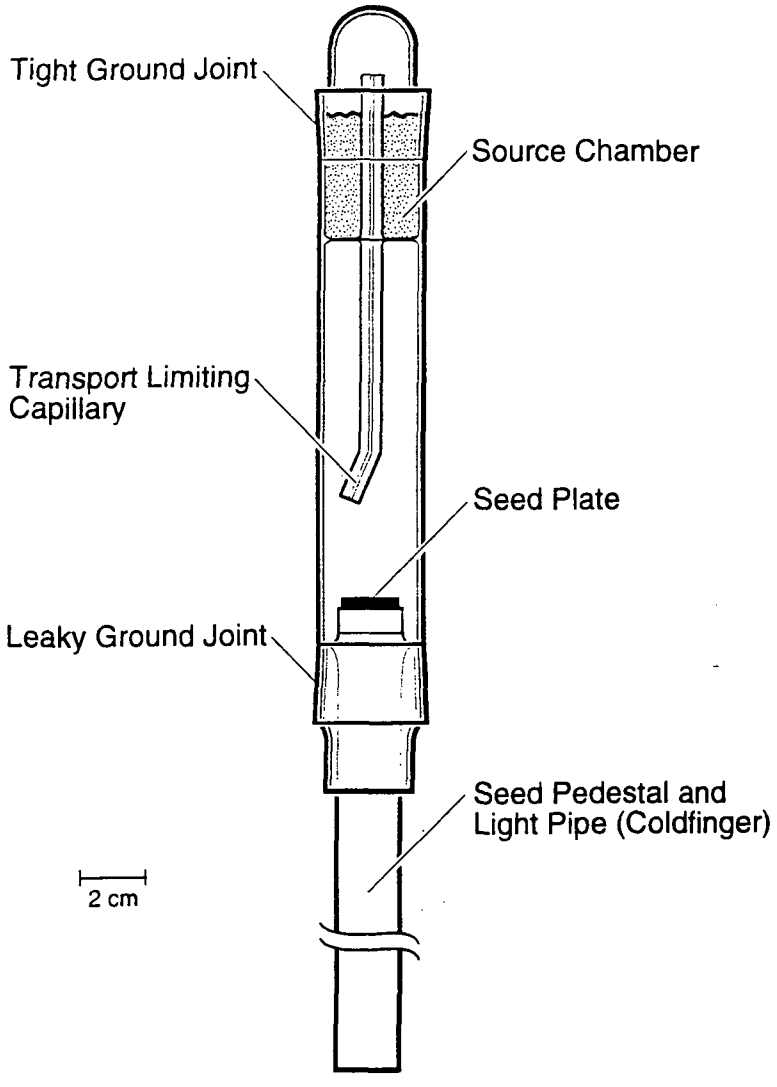

Fig. 2. Ampoule for effusive physical vapor transport

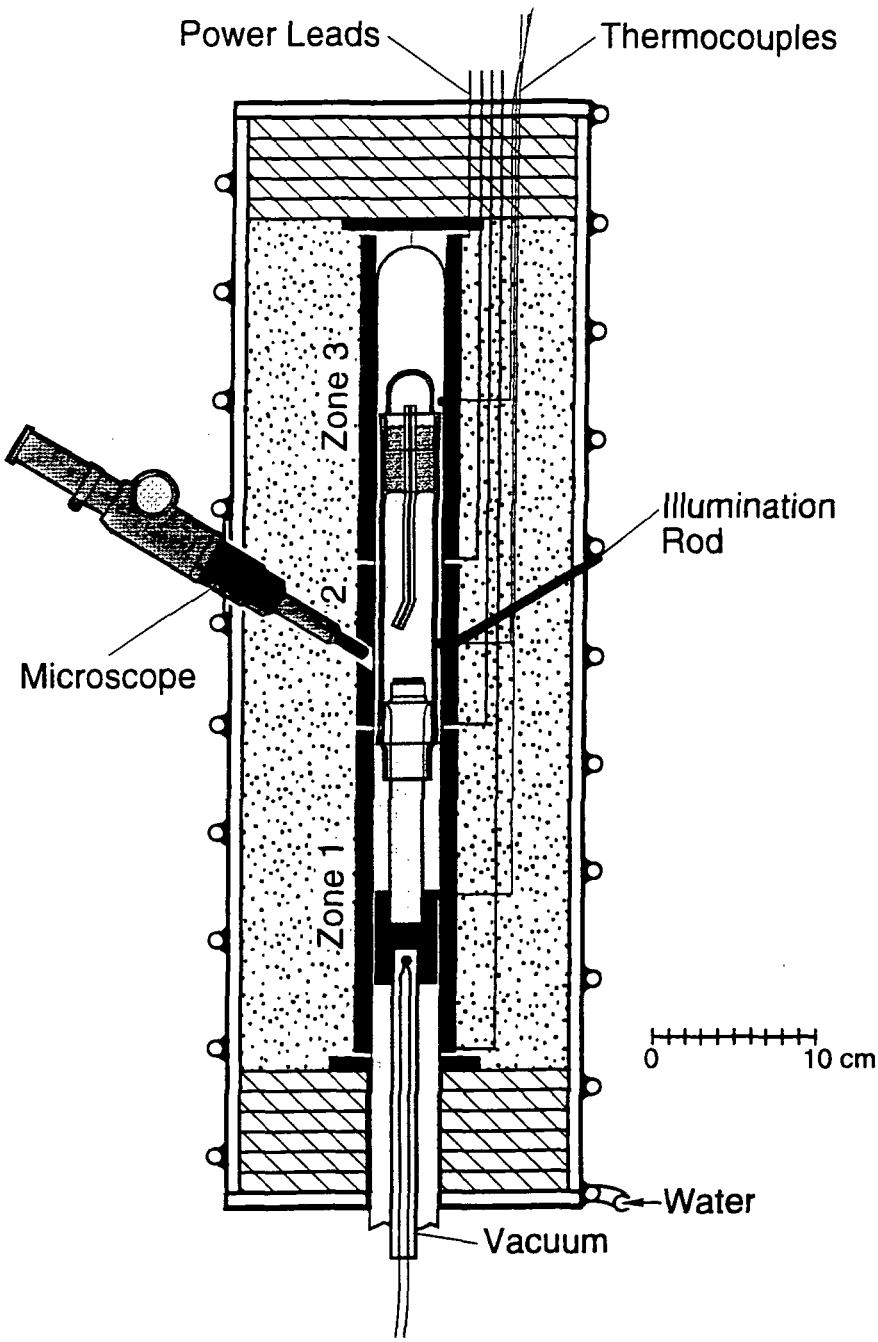

Fig. 3. Cross-section of three-zone furnace for effusive ampoule vapor transport with high temperature microscope for observation of epitaxial growth on seeds.

4. Results and Discussion

Some runs were conducted with zinc selenide in the effusive ampoule system. Results were promising. Seeds were obtained from the earlier physical vapor transport growth experiments. Growth rates were 2-3 mm/day at 1050-1100 °C, with lower temperatures producing polycrystals. The crystals produced at 1100 °C grew epitaxially, with no new twins on the seed boundaries. Growth rates in the closed system physical vapor transport system were roughly 1 mm/day.

As indicated in Sect. 2.5, it was then decided to grow cadmium telluride crystals instead of zinc sulfoselenide crystals. The cadmium telluride and zinc sulfoselenide have sphalerite crystal structures and the systems are very similar, as both are very prone to twinning and would have sphalerite-wurtzite phase transitions at roughly the same temperatures (if cadmium telluride wasn't a liquid at 1100-1200 °C). In both materials the critical resolved shear stress and stacking fault energies are very low. But the cadmium telluride system is much easier to work with than either zinc sulfide or zinc sulfoselenide, and much more is known about characterization methods for cadmium telluride.

Hence, it was decided to work on growth of the various faces of cadmium telluride. This insight will also be applicable to zinc selenide and zinc sulfide. The faces selected for growth rate tests were {100}, {110}, {111}, {211} and {511}. {111}, {211} and {511} planes have both either cadmium-rich (A) and tellurium-rich (B) faces. Each face was run under identical growth conditions.

The variations in growth between the various faces have been substantial. {110} seeds grow well laterally. The large facets on the {110} face reveal the slower vertical growth of this face. Greater supersaturation required for vertical growth is shown by the need for a temperature gradient up to 5°C greater for {110} faces to prevent parasitic nucleation on the ampoule walls. The {100} and near {100} faces twinned easily into faces that quickly crowded them out. {211} faces grew well upward, but had problems crowding out other faces that resulted from second-order twinning during lateral growth. The {111} and especially {511} faces produced crystals that both grew laterally and vertically without expanding twins, if the B face was up. Twins grew inward and expanded if the A face was placed upward.

CdTe twins around {111} axes, producing twin boundaries that run along {211} axes, as can be seen in the {011} plane projection of Figure 4. So twinning around {111} axes during lateral growth (seed spreading) produces twins that do not grow or shrink during growth in a perpendicular {211} direction, as long as these twins do not experience second- or third- order

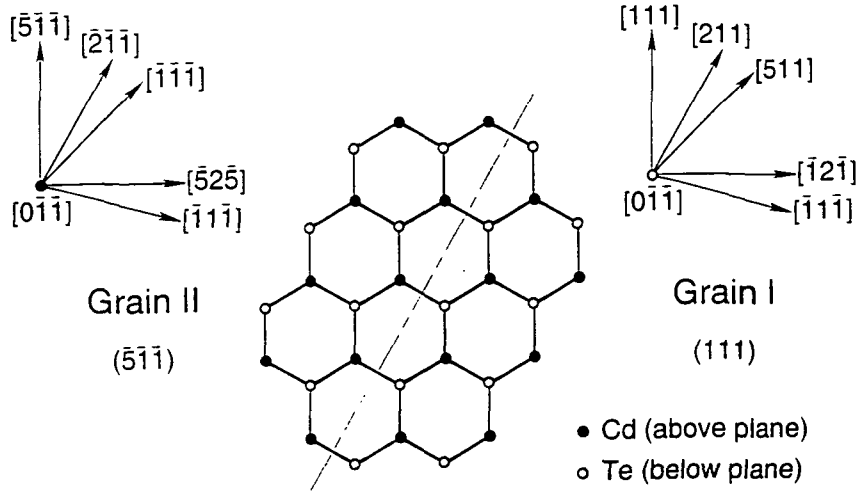

Fig. 4. Projection into the $(0\bar{1}\bar{1})$ plane of twin (grain II) and matrix (grain I) domains for CdTe with a [111] growth axis. The twin is produced by rotation around the $[\bar{1}1\bar{1}]$ axis.

twinning. {n11} planes (with n>2) are set up so that twins grow outward unless interstitials allow the twin to be blocked off by a regrowth of the main boule. This does not occur on the A faces and for faces around {100}.

Viewing of cadmium telluride crystals during growth shows that the transition between growth with twinning and high dislocation densities to more epitaxial growth around 850 °C is just a function of the growth rate. Crystals round below 850 °C just as they do above 850 °C, but much more slowly. Growth without twins and high dislocation densities is possible below 850 °C, but the maximum growth rate is so slow as to make this impractical. The difference between growth and etching at these speeds is not easily distinguishable.

Photoluminescence measurements were made of one of these crystals. The bottom portion was 4° off {100}, while the top was roughly {411}. These curves show that the top portion of the crystal has fewer impurities than the seeded section on the bottom, as the bottom piece has a varying number of impurities. The CdTe seed is one of those obtained from II-VI, Inc. The II-VI seeds were used for the early growth experiments, while seeds from the early growth runs were used for the later growth runs. While the II-VI seeds have more impurities, more twins were detected on lateral growth with the self-cut seeds. Typical etch-pit densities for

these crystals were $1\text{-}3\times10^{-3}/cm^2$.

We searched for the sub-micron diameter tellurium precipitates that are said to be in all cadmium telluride due to stoichiometry changes during cooling. One part of this search involved the use of an atomic force microscope (AFM). Several cadmium telluride samples were used, and prepared differently. The first was polished to 0.3 μm with aluminum oxide, then rinsed in distilled water and methanol. This sample was too rough and had too many particles on the surface (identified as oxide particles). The next sample was polished to 0.05μm with aluminum oxide, then ultrasonically cleaned in distilled water for several minutes. The surface was smoother, with much fewer oxide particles. The remaining scratches on the surface (approximately 50 nm wide) were oriented in {110} directions. A number of features on the surface appeared to be possible Te precipitates.

The next sample was polished and cleaned as the second sample, but then was etched in a 5% bromine in methanol solution for 5 minutes. Observation under the sighting microscope of the AFM showed some etch pits of 1-5μm diameter. However, the smaller features did not show any etch pit holes that would be expected if the small features were tellurium or cadmium deposits [40]. The surfaces were nearly identical to those observed for the last sample. Allowing these samples to sit in air for even a few days led to roughening of the surface and the appearance of more and larger features. These features appear to be cadmium or tellurium oxides. A typical sample is depicted in Figures 5 and 6.

Differential thermal analysis (DTA) was also used in searching for these precipitates. First, a very small amount of tellurium was run to establish tellurium melting and freezing points along the DTA heating and cooling curves. Several CdTe samples were used: One of Cerac 5N CdTe that had a large number of impurities, one of this same material transported once under vacuum at 700-750 °C, and a sample from the source material for growing the crystal. The untreated Cerac material showed peaks similar to Te melting under static air conditions, but no such peaks were visible for any of the samples run under flowing argon. All samples run under flowing argon showed the same traces. Either the small precipitates did not exist in large numbers, or they did not melt at the same temperatures.

5. Conclusions

This work has shown that the {n11} Te-rich growth faces work best for CdTe in the effusive ampoule growth system. It has also demonstrated the suitability of ZnSe crystal growth in this system at roughly 1050 °C. Selenium-rich zinc sulfoselenide could be grown by the same method with the addition of a selenium or sulfur reservoir to keep the sulfur to selenium ratio

constant. No submicron diameter tellurium precipitates were detected in the CdTe crystals,by atomic force microscopy of crystal sections.

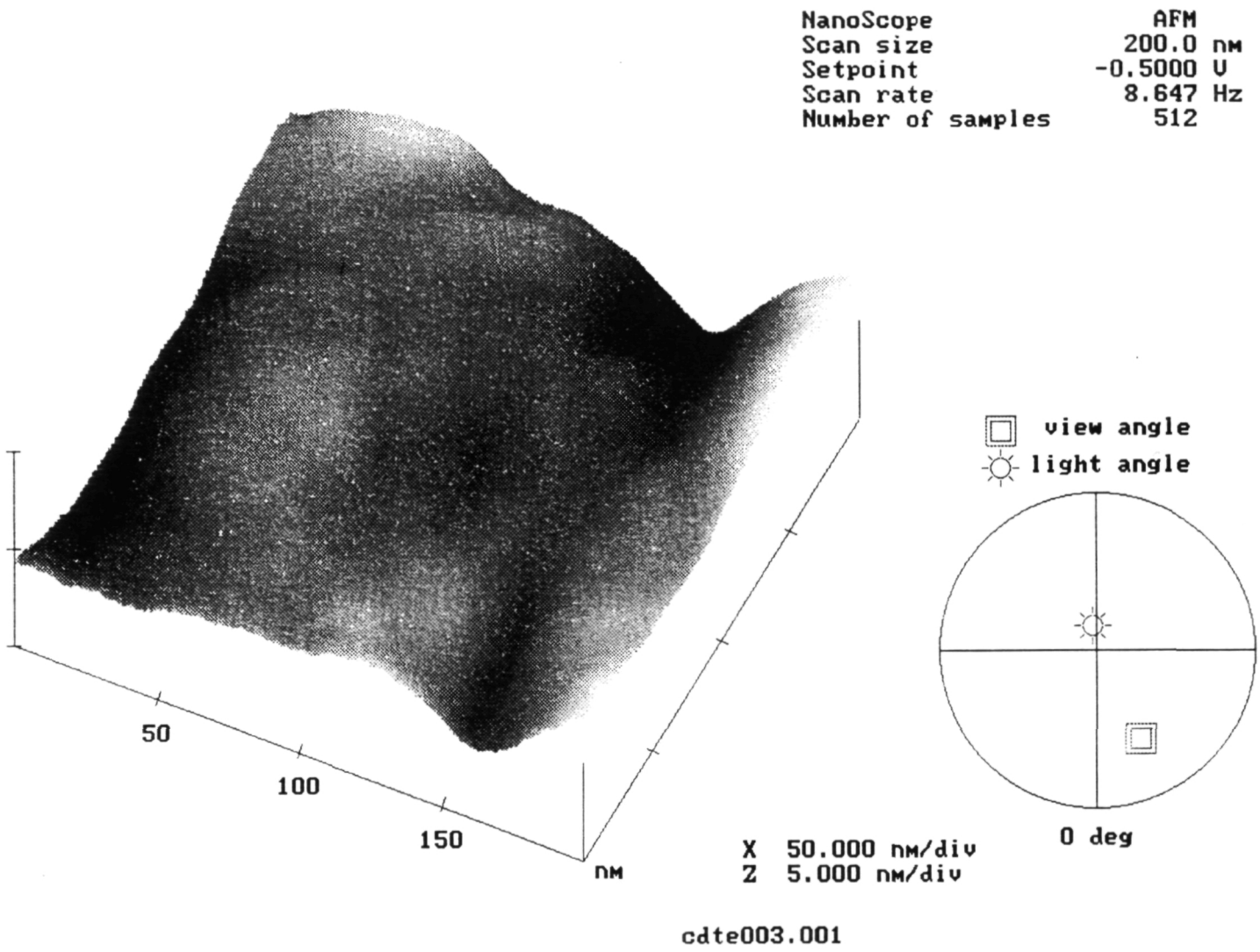

Figure 5. Height map of CdTe sample measured by atomic force microscopy.

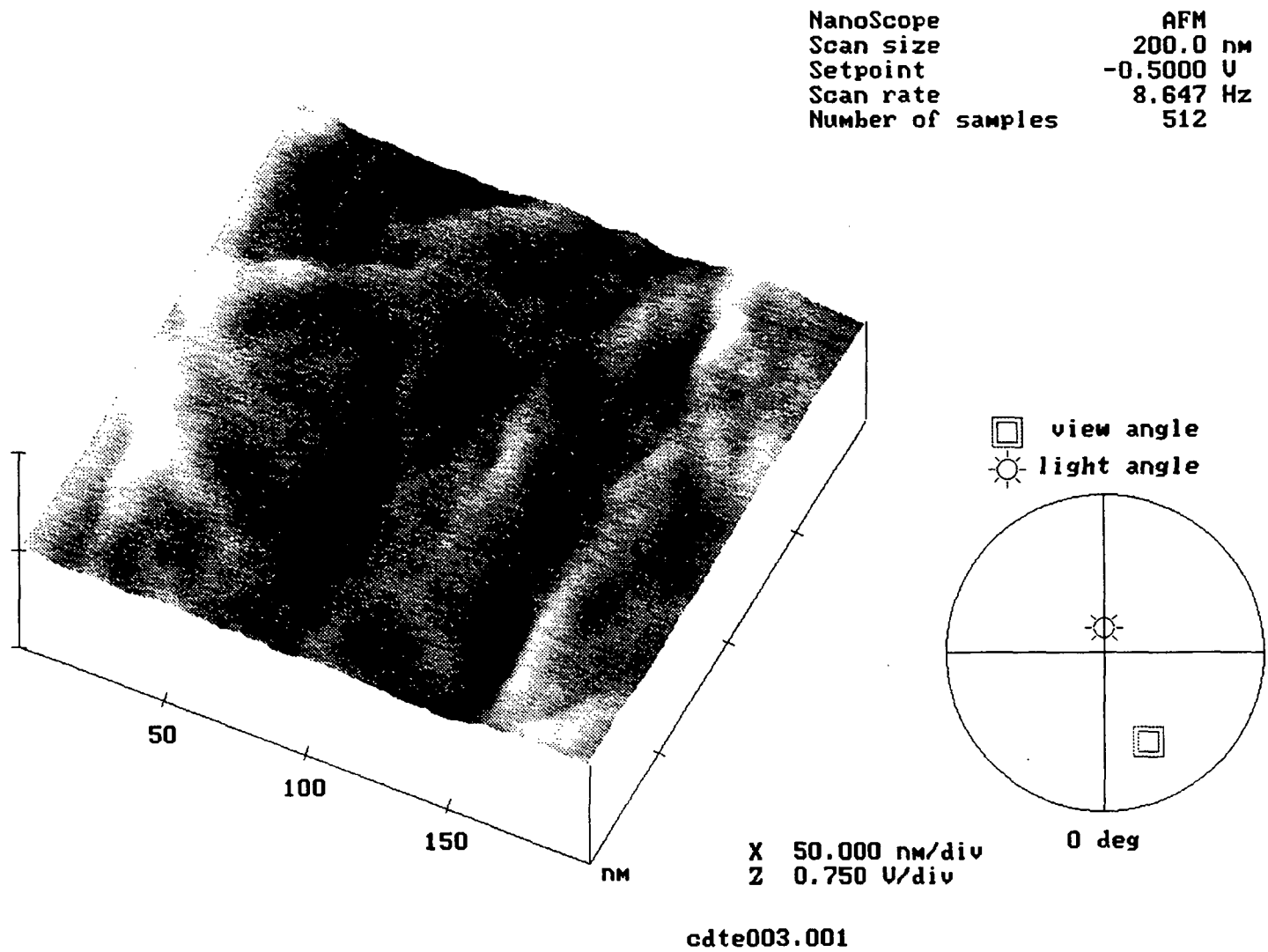

Figure 6. Torque map of CdTe sample obtained with atomic force microscope. Torque changes indicate either a change in the slope of the surface or a change in surface composition. All changes appear to be correlated with changes in the slope of Figure 5 (height map). Hence, there are no apparent composition changes that could be interpreted as precipitates.

References

[1] R. A. Reynolds, *The II-VI compounds: 30 years of history and the potential for the next 30 years*, J. Vac Sci. Tech. A **7** (1989) 269.

[2] X. H. Yang et al., *Two-photon pumped blue lasing in bulk ZnSe and ZnSSe,* Appl. Phys. Lett. **62** (1993) 1071.

[3] X. H. Yang et al., *Room temperature blue lssing of ZnS_xSe_{1-x} alloys by photopumping,* Appl. Phys. Lett. **60** (1992) 926.

[4] C. Chung, F. Jain and G. Drake, *Prospects of fabricating blue-green lasers using ZnSe based metal-insulator-semiconductor (MIS) heterostructures*, J. Crystal Growth **117** (1992) 1062.

[5] R. N. Bhargava, *Compact blue lasers in the near future*, J. Crystal Growth **117** (1992) 894.

[6] H. Katayama-Yoshida, T. Saski and T. Oguchi, *Theory of the self-compensation in p-type ZnSe*, J. Crystal Growth **117** (1992) 625.

[7] R. M. Park, H. A. Mar and N. M. Salansky, *Homo- and heteroepitaxial growth of high quality ZnSe by molecular beam epitaxy*, J. Vac. Sci. Tech. B **3** (1985) 1637.

[8] M. Kolodziejczyk et al., *The likelihood of III_2-VI_3 compound formation during epitaxial growth of II-VI on III-V semiconductors,* J. Crystal Growth **117** (1992) 549.

[9] Y. Tomomura, M. Kitagawa, A. Suzuki and S. Nakajima, *Homoepitaxial growth of ZnS single crystal thin films by molecular beam epitaxy*, J. Crystal Growth **99** (1990) 451.

[10] T. Koyama et al., *Growth of ZnSe single crystals by iodine transport*, J. Crystal Growth **91** (1988) 639.

[11] J. R. Cutter and J. Woods, *Growth of single crystals of zinc selenide from the vapour phase*, J. Crystal Growth **47** (1979) 405.

[12] X. M. Huang and K. Igaki, *Growth and exciton luminescence of ZnSe and ZnS_xSe_{1-x}* , J. Crystal Growth **78** (1986) 24.

[13] V. A. Kuznetsov, *The physical chemistry of the hydrothermal crystal growth and the crystallization of some A^2B^6 crystals,* Prog. Crystal Growth and Charact. **21** (1990) 163.

[14] G. Cantwell et al., *Growth and characterization of substrate-quality ZnSe single crystals using seeded physical vapor transport*, J. Appl. Phys. **71** (1992) 2931.

[15] M. P. Kulakov and I. V. Balyakina, *Solid state wurtzite-sphalerite transformation and phase boundaries in ZnSe-CdSe*, J. Crystal Growth **113** (1991) 653.

[16] K. Terashima and M. Takena, *Typical macroscopic defects in ZnSe crystals grown from the melt*, J. Crystal Growth **110** (1991) 623.

[17] H. Yoshida, T. Fujii, A. Kamata and Y. Nakata, *Undoped ZnSe single crystal growth by*

the vertical Bridgman method, J. Crystal Growth **117** (1992) 75.

[18] T. Koyama, T. Yodo and K. Yamashita, *Crystallographic properties of ZnSe grown by sublimation method*, J. Crystal Growth **94** (1989) 1.

[19] H. Y. Cheng and E. E. Anderson, *The growth of ZnSe single crystals by physical vapor transport*, J. Crystal Growth **96** (1989) 756.

[20] W. Palosz, *Growth of ZnS and $Zn_{1-x}Cd_xS$ ($x \leq 0.07$) single crystals by iodine transport*, J. Crystal Growth **60** (1982) 57.

[21] A. Catano and Z. K. Kun, *Growth and characterization of ZnSe and homogenous ZnS_xSe_{1-x} crystals*, J. Crystal Growth **33** (1976) 324.

[22] S. Satoh, M. Isshiki and K. Igaki, *Electrical properties of ZnSe*, Japan. J. Appl. Phys. **22** (1983) 1167.

[23] H. Samuelson, *Vapor phase growth and properties of zinc sulfide single crystals*, J. Appl. Phys. **32** (1961) 309.

[24] H. Samuelson, *Growth of cubic ZnS single crystals by a chemical transport process*, J. Appl. Phys. **33** (1962) 1779.

[25] W. Palosz, M. J. Kozielski and B. Palosz, *Dependence of the structure on the growth conditions of ZnS and $Zn_{1-x}Cd_xS$ single crystals grown by iodine transport*, J. Crys. Growth **58** (1982) 185.

[26] W. L. Garrett, G. Ruban and F. Williams, *Anisotropy and twinning in cubic zinc sulfide crystals*, J. Chem. Solids **43** (1982) 497.

[27] J. R. Cutter, G. J. Russell and J. Woods, *The growth and defect structure of single crystals of zinc selenide and zinc sulpho-selenide*, J. Crys. Growth **32** (1976) 179.

[28] G. J. Russell and J. Woods, *Vapour growth and defect characterization of large single crystals of ZnS and Zn(S,Se)*, J. Crys. Growth **47** (1979) 647.

[29] S. Mardix, *Polytypism: a controlled thermodynamic phenomenon*, Phys. Rev B **33** (1986) 8677.

[30] S. Mardix, *Crystallographic aspects of polytypism in ZnS*, Bull. Mineral. **109** (1986) 131.

[31] E. T. Allen and J. R. Crenshaw, Am. J. Sci. **34** (1912) 341.

[32] J. Baars and G. Brandt, *Structural phase transitions in ZnS*, J. Phys. Chem. Solids **34** (1973) 905.

[33] K. Young, A. Kahn and J. M. Phillips, *(511) and (711) GaAs epilayers prepared by molecular-beam epitaxy*, J. Vac. Sci. Tech. B **10** (1992) 71.

[34] G. H. Olsen, T. J. Zamerowski and F. Z. Hawrylo, *Vapor growth of InGaAs and InP on (100), (110), (111), (311) and (511) InP substrates*, J. Crys. Growth **59** (1982) 654.

[35] D.W. Greenwell, B.L. Markham and F. Rosenberger, *Numerical modeling of diffusive Physical Vapor Transport in Cylindrical Ampoules*, J. Crystal Growth **51** (1981) 413.

[36] B. L. Markham, D. W. Greenwell and F. Rosenberger, *Numerical modeling of diffusive-convective physical vapor transport in cylindrical vertical ampoules*, J. Crystal Growth **51** (1981) 426.

[37] J. R. Abernathey, D. W. Greenwell and F. Rosenberger, *Congruent (diffusionless) vapor transport*, J. Crystal Growth **47** (1979) 145.

[38] F. Rosenberger, M. Banish and W. M. B. Duval, *Vapor crystal growth technology development - Application to cadmium telluride,* NASA Technical Memorandum

[39] R. M. Banish, *Effusive ampoule physical vapor transport and application to cadmium telluride,* Ph. D. Thesis, Dept. of Materials Science and Engineering, University of Utah (1992).

[40] J. Shen et al., *Etch pits originating from precipitates in CdTe and* $Cd_{1-x}Zn_xTe$ *grown by the vertical Bridgman-Stockbarger method*, J. Crys. Growth **132** (1993) 351.